

# Simple and Economical Method for the Preparation of MgO Nanostructures with Suitable Surface Area

*Alaei, Mahshad\*<sup>+</sup>; Jalali, Mona; Rashidi, Alimorad*

*Catalysis & Nanotechnology Research Division, Research Institute of Petroleum Industry (RIPI),  
P.O. Box 14665-1998 Tehran, I.R. IRAN*

**ABSTRACT:** *A facile and simple method was proposed to control the size and shape of the MgO nano structures with high surface area in the presence of efficient and cheap templates like PEG 200, PEG 600, PEG 4000 and sorbitol at low temperature within a little time. Nano rods and Nanoparticles have been achieved by applying these templates and altering other growth parameters. The products were characterized by X-Ray Diffraction (XRD), Scanning Electron Microscopy (SEM), Transmission Electron Microscopy (TEM) and Thermo Gravimetric Analysis (TGA). The surface area of the samples was characterized by BET method. The effect of the growth parameters such as template, pH, Mg<sup>2+</sup>/template, molar ratio and temperature on the growth and morphology of MgO nano structures have been investigated in details. By tuning these parameters MgO nano rods and nano particles can be formed.*

**KEY WORDS:** *Magnesium oxide, Nanoparticles, Nanorods, Co-precipitation method.*

## INTRODUCTION

Metal oxides such as magnesium oxide (MgO) are extremely important technological materials for use in catalyst, catalyst support, electronic and photonic devices. The magnesium oxide (MgO) is a very suitable material for insulation applications because of their low heat capacity and high melting point [1]. Nano MgO is a functional material that has been widely used in various areas [2,3]. MgO has a good bactericidal performance in aqueous environments due to the formation of superoxide (O<sub>2</sub><sup>-</sup>) anions on its surface [4,5]. *Klabunde & Coworkers* demonstrated that nano-MgO exhibits high activity against bacteria, spores and viruses after adsorption of halogen gases due to its large surface area, abundance in crystal defects and positively-charged particles which

can result in strong interactions with negatively-charged bacteria and spores [6-8]. During the past several years, various methods have been developed for the synthesis of nanomaterials that have included template-assisted [9], Vapor-Liquid-Solid (VLS) [10], colloidal micelles [11], electrochemical processes [12], ultrasonic method [13] and domestic microwave oven [14].

In the present study, we report a simple and inexpensive synthesis route of MgO nanostructures by co-precipitation method. We have studied the effect of different reaction parameters such as temperature, pH, kind of template and molar ratio of precursor and template on the product morphology.

---

\* To whom correspondence should be addressed.

+ E-mail: [alaiem@ripi.ir](mailto:alaiem@ripi.ir)

1021-9986/14/1/21

8/\$/2.80

**Table 1: Reaction conditions samples of the as-prepared MgO nanostructures.**

Sample	Mg <sup>2+</sup> /template molar ratio	Kind of template	pH	Temperature (°C)	Structure
NO. 1	2	PEG 200	10	70	Agglomerated particles
NO. 2	2	PEG 600	10	70	Nanorod
NO. 3	2	PEG 200	9	70	Agglomerated particles
NO. 4	4	PEG 200	10	70	Agglomerated particles + nanoparticle
NO. 5	2	PEG 200	11	70	Nanoparticle
NO. 6	2	PEG 200	10	60	Agglomerated particles +nanorod
NO. 7	2	Sorbitol	10	70	Agglomerated particles + nanoparticle
NO. 8	2	PEG 200	10	80	Agglomerated particles
NO. 9	2	PEG 4000	10	70	Agglomerated particles + nanoparticle
NO. 10	1	PEG 200	10	70	Nanoflake

## EXPERIMENTAL SECTION

### Materials and Characterization

All chemicals such as Mg(NO<sub>3</sub>)<sub>2</sub>.6H<sub>2</sub>O, polyethylene glycol 200 (PEG200), polyethylene glycol 600 (PEG 600), polyethylene glycol 4000 (PEG 4000), sorbitol and ammonia were of analytical grade and used without further purification.

The sample was characterized by Scanning Electron Microscopy (SEM) using a Holland Phillips XL30 microscope. XRD patterns of the samples were recorded in ambient air using a Holland Philips X-ray powder diffraction (Cu K $\alpha$ ,  $\lambda=1.5406 \text{ \AA}$ ), at scanning speed of 2°/min from 20° to 80°. TEM images of the samples as prepared by Philips Analytical equipment (80 kV). Surface area of the desired sample was determined by Belsorp adsorption-desorption (BEL Japan Inc.).

TGA (TA Instruments 951) of the samples was used to study the removal of water, CO<sub>2</sub> and the fuels residual carbonaceous species. A heating rate of 10°C/min was used for TGA measurements up to 800°C in air.

### Preparation of MgO nanostructures

An appropriate amount of Mg(NO<sub>3</sub>)<sub>2</sub>.6H<sub>2</sub>O was dissolved in 300 mL distilled water in order to form 0.012 M solution (Solution A). Different quantities of template (PEG 200, PEG 600, PEG 4000 and sorbitol) was added separately to the desired amount of NH<sub>3</sub>-H<sub>2</sub>O and well mixed by stirring for 5 min. The as-prepared solution was added drop wise to the solution A at room temperature under stirring. The mixture was heated

to reaction temperature of 60, 70 or 80°C and kept for few minutes. Experiments were carried out in different molar ratios of Mg<sup>2+</sup> source/template including 1, 2, and 4 while the pH value was adjusted in 10 during the reaction time. As the reaction completed, the as-prepared white solid products were washed with distilled water and ethanol to remove the ions possibly remaining in the final products, and finally dried at 60°C overnight. The product was calcined at 550 °C for 2h. To study the effect of other growth parameters on morphology and size of the MgO nanostructures, reaction parameters such as kind of template, different molar ratios of Mg<sup>2+</sup> source/template, pH and temperature were tuned during the synthesis to obtain the desired morphology and size of MgO nanostructures that can be used for different applications.

## RESULTS AND DISCUSSIONS

### Effect of template and Mg<sup>2+</sup>/template molar ratio

Table 1 depicts the experimental conditions studied to achieve a controllable growth of MgO nanostructures by finding the most effective parameters. Figs. 1 and 2 show the XRD patterns of the ten as-prepared MgO nanostructures. All the diffraction peaks can be indexed to face-centered cubic phase of MgO (JCPDS 87-0653) with a preferred orientation along the (200) direction. The sharp diffraction peaks indicate the good crystallinity of the prepared MgO powders.

PEG 200, PEG 600, PEG 4000 and sorbitol were examined as template in the similar experimental conditions. The formation of MgO nanostructures

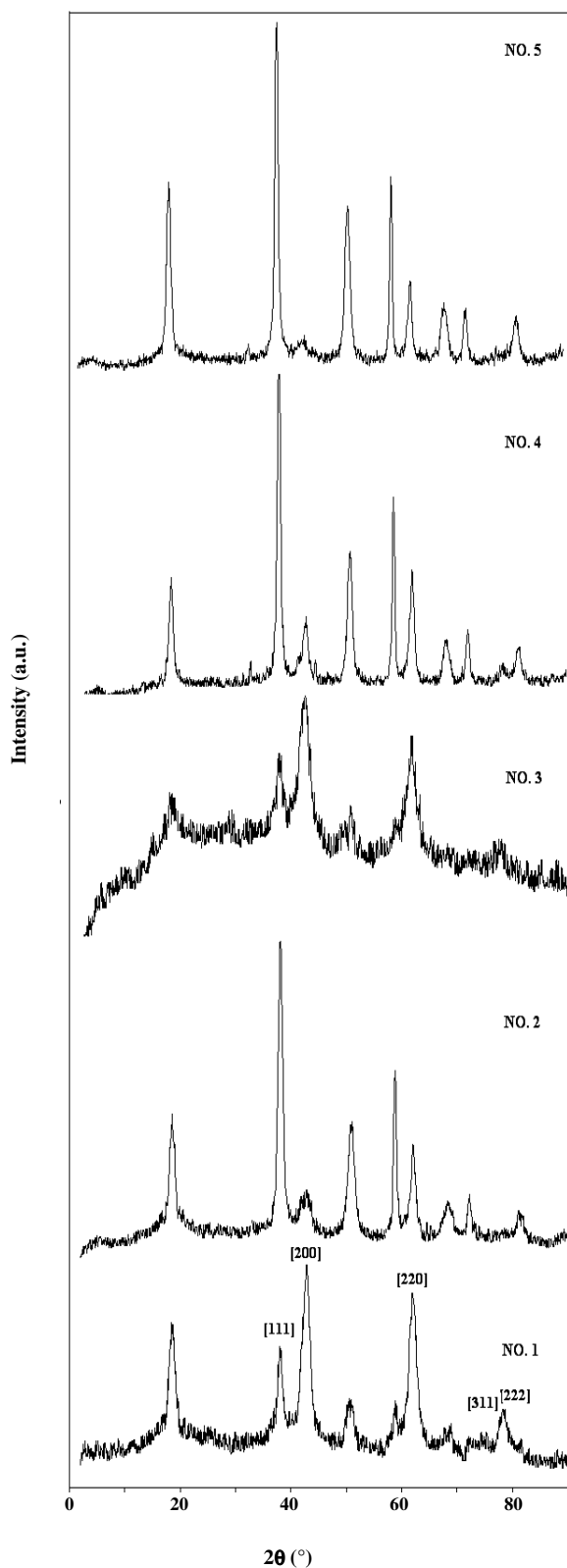


Fig. 1: XRD patterns of the as-prepared MgO nanostructures (samples 1,2,3,4,5).

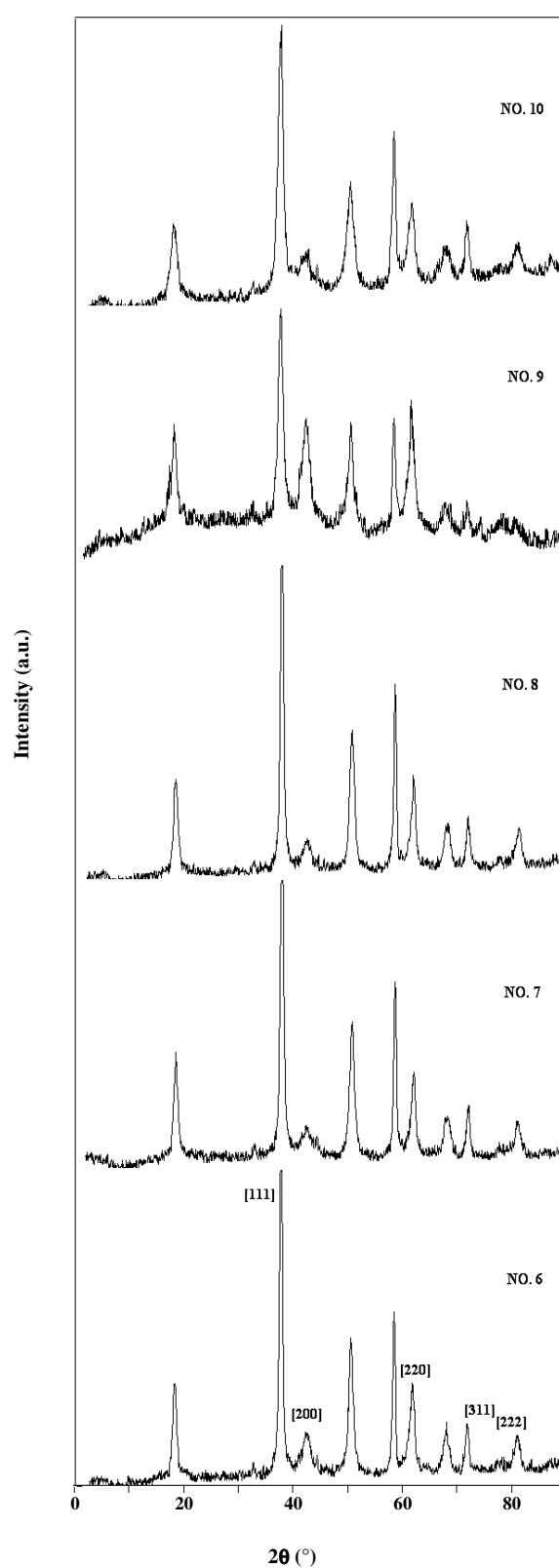


Fig. 2: XRD patterns of the as-prepared MgO nanostructures (samples 6,7,8,9,10).

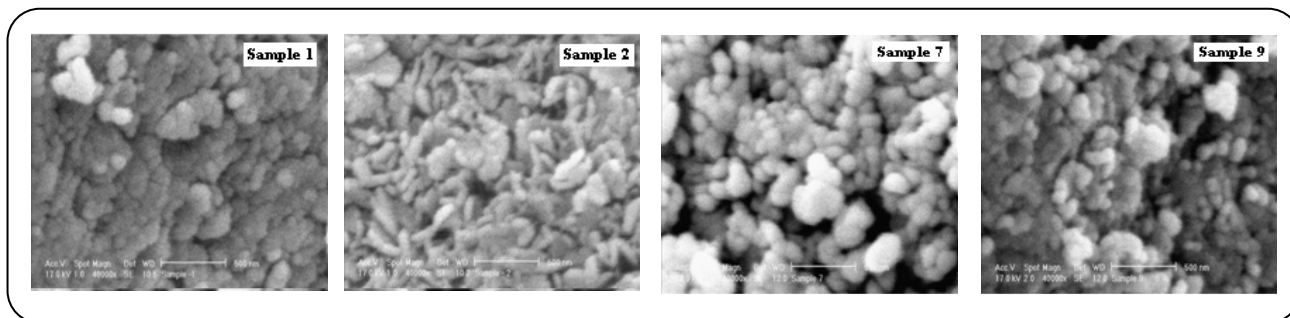


Fig. 3: SEM images of the as- prepared MgO nanostructures (samples 1,2,7,9) that were prepared with different template (PEG 200, PEG 600, Sorbitol and PEG 4000 respectively).

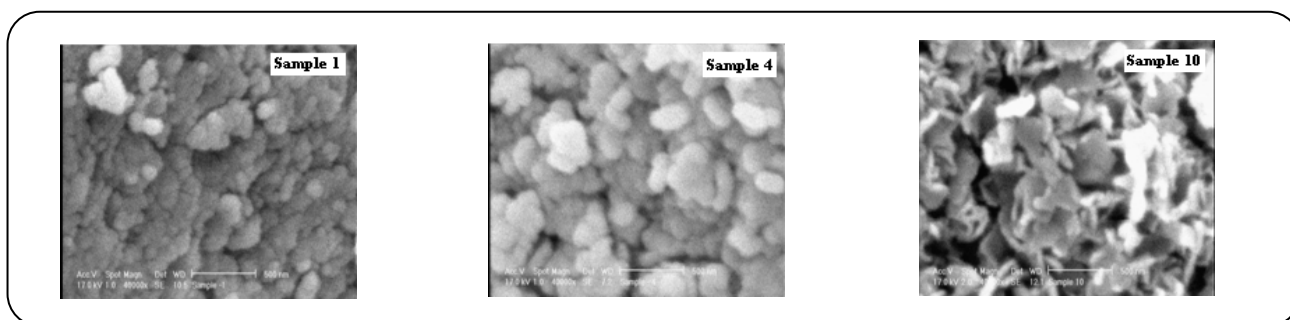


Fig. 4: SEM images of the as- prepared MgO nanostructures (samples 1,4 ,10) with different  $Mg^{2+}$ /template molar ratio (2,4 and 1 respectively).

may be due to the creation of nuclei by the addition of template firstly [14]. Fig. 3 indicates that the variation of template can alter the morphology of MgO nanostructures. In this figure, the SEM images of samples 1,2,7,9 with PEG 200, PEG 600, Sorbitol and PEG 4000 as templates respectively were compared with each other. Sample 2 has well defined nanorod structure. The mixture of agglomerated particles and nanoparticles can be seen in SEM images of samples 7,9. Nanoparticles rarely exist among of agglomerated particles in Sample 1.

As a result, polymeric glycols (poly ethylene glycol) with optimum Molecular weight (PEG 600) will be very suitable template for the preparation of MgO nanorods with this method. High molecular weight of PEG 4000 causes stereo stric problems while PEG 200 and sorbitol with low molecular weight cannot be the suitable template for the formation of MgO nanorods.

In order to investigate controllable growth of MgO nanostructures, different  $Mg^{2+}$  source/template ratios were used, employing PEG 200 as template. Fig. 4 indicates that the different  $Mg^{2+}$  source/template ratios can alter the morphology of MgO nanostructures. In this figure, the SEM images of samples 1,4 ,10 with  $Mg^{2+}$

source/template ratios of 2, 4 and 1 respectively were compared with each other. Sample 10 has well defined nanoflake structure. The mixture of agglomerated particles and nanoparticles can be seen in SEM images of sample 4. Nanoparticles rarely exist among of agglomerated particles in Sample 1. It is concluded that controllable reaction condition can be achieved by using low concentration of precursor.

#### Effect of reaction temperature

It is expected that by increasing the temperature reaction, the average particle size of the products will be increased [15]. Fig. 5 indicates that the different temperature reaction can alter the morphology of MgO nanostructures. In this figure, the SEM images of samples 1,6 and 8 with temperature reaction of 70,60 and 80°C respectively were compared with each other. The mixture of agglomerated particles and nanorods can be seen in SEM images of sample 6. Nanoparticles rarely exist among of agglomerated particles in Samples 1 and 8. At 60°C, a mixed morphology of MgO nanorod/nanoparticle has formed. When the reaction temperature increased, the rods became thicker and shorter; in contrast, when

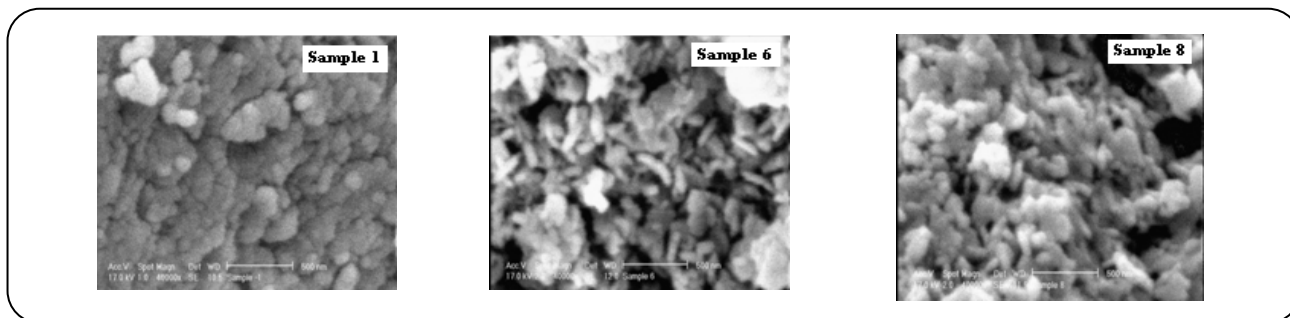


Fig. 5: SEM images of the as- prepared MgO nanostructures (samples 1, 6, 8) with different temperature reaction (70, 60 and 80 °C respectively).

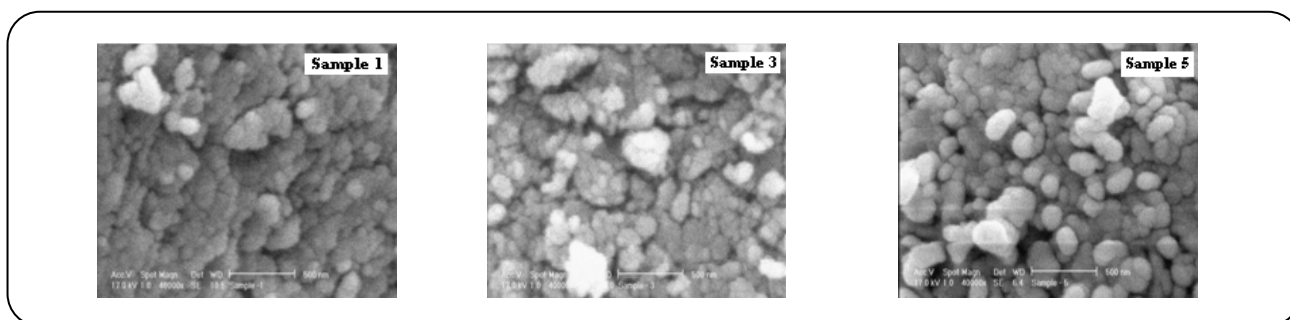
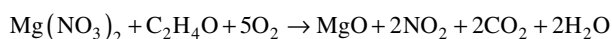
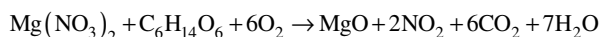
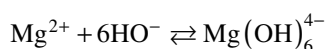
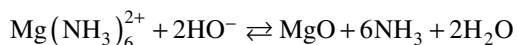
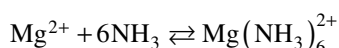
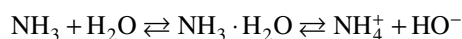


Fig. 6: SEM images of the as- prepared MgO nanostructures (samples 1, 3, 5) with different pH (10, 9 and 11 respectively).

the reaction was performed at a higher temperature (85°C), the morphology inclined to porous structure. In order to verify the temperature effect on morphology, the possible reactions in an aqueous solution can be expressed as follows:



It can be seen that MgO nuclei are obtained by the dehydration of  $\text{Mg}(\text{OH})_6^{4-}$  or  $\text{Mg}(\text{NH}_3)_6^{2+}$ . It is expected that adsorption of ions on the substrate will play an important role in determining the particle size. It is understood that at lower temperatures there is a high

density of adsorbed nuclei and at higher temperatures the density of nuclei on the substrate is much less.

It is seen that bigger particles are formed on increasing the temperature. Therefore, for lower density of nuclei (higher temperature) the crystal grows larger in size before being blocked (the possibility of getting blocked is low), in comparison to the situation where a high density of nuclei (lower temperature) results in small crystals before being blocked. The higher density of nuclei enhances the possibility of a crystal to get blocked [16].

### Effect of pH

pH was found to be an important parameter affecting MgO nanostructures synthesis.

Fig. 6 presents that the variation of pH can alter the morphology of MgO nanostructures. In this figure, the SEM images of Samples 1, 3 and 5 with pH=9, 10, 11 respectively were compared with each other. Sample 5 has well defined nanoparticle structure. Nanoparticles rarely exist among of agglomerated particles in Samples 1 and 3. We suppose that the excess amount of  $\text{OH}^-$  ions in the preparation condition of sample 5 may cause homogenous formation of Magnesium hydroxide nucleus with the least agglomeration.



Fig. 7: TEM images of sample 2 with nanorod structure.

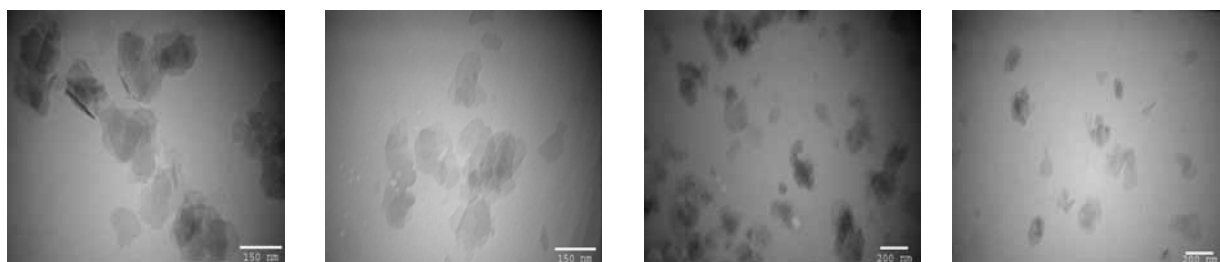


Fig. 8: TEM images of sample 5 with nanoparticle structure.

As can be seen, Samples 2 and 5 have well defined and homogenous nanostructures (nanorod and nanoparticle morphology respectively) among of the as-prepared samples. The further characterization of these samples is performed by TEM. Fig. 7 indicates TEM images of Sample 2 that presents well defined nanorod structure. These images were agreed with the result of related SEM image. Fig. 8 presents TEM images of Sample 5 that indicates well defined nanoparticle structure and were agreed with the result of related SEM image. The average particle size of the nanoparticles in Sample 5 is about 50 nm (in comparison to the previous research that was reported 72.4 nm [13]). The average particle size can be calculated from XRD pattern by the Debye-Scherrer formula.

$$D_{hkl} = \frac{0.89\lambda}{(\beta \cos \theta)}$$

Where the  $\lambda$  is X-ray wavelength (0.1540 nm for Cu-K $\alpha$ ),  $\beta$  is the width at half maximum of the diffraction peak and  $\theta$  is Bragg diffraction angle.

Surface area of the Samples 2 and 5 was determined by Belsorp adsorption-desorption (BET) method at 480 °C. The related results are 176 and 231 m<sup>2</sup>/g for Samples 2 and 5 respectively. In comparison to the similar previous

researches and by considering the calcinations temperature [17], Samples 2 and 5 have very suitable and high surface area.

Fig. 9 indicates TGA curves of the Samples 2 and 5 that was used to study the thermal behavior of the samples. A heating rate of 10°C/min was used for TGA measurements up to 800°C in air. The weight loss that is observed for the Sample 2 and 5 in the temperature range of 300-380 °C, can be attributed to the decomposition of Mg(OH)<sub>2</sub> [18].

## CONCLUSIONS

In conclusion, a simple and economical method was successfully utilized for the synthesis of MgO nanorods (Sample 2) and nanoparticles (Sample 5) with high surface area (176 and 231 m<sup>2</sup>/g respectively). Effective reaction parameters were investigated in detail. Variation of template and pH can alter the morphology of MgO nanostructures. By using PEG 600 at pH=10, Sample 2 with nanorod structure and by using PEG 200 at pH=11, Sample 5 with nanoparticle structure have been prepared.

Also variation of temperature and Mg<sup>2+</sup>/template molar ratio can alter the morphology of the samples. Therefore by tuning the reaction parameters, we can obtain different morphology of MgO nanostructures by this method.

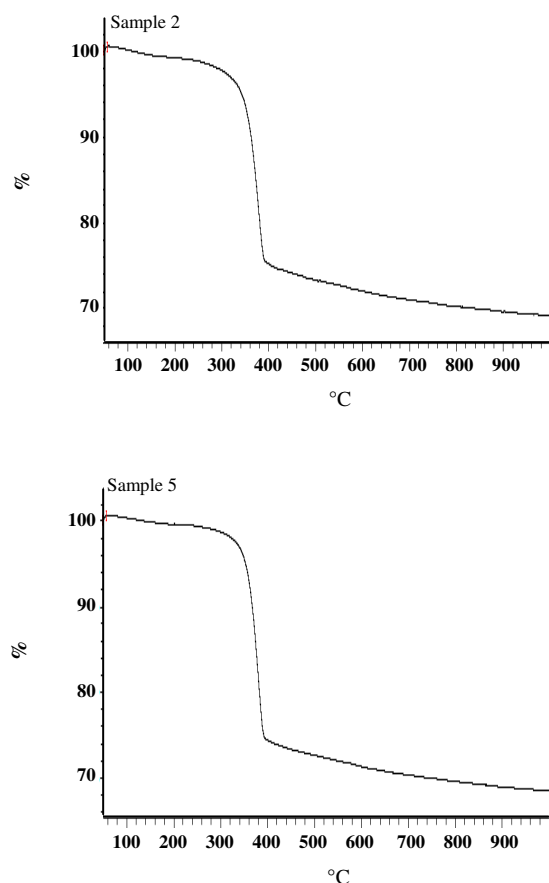


Fig. 9: Sample 2,5 TGA analysis.

### Acknowledgement

This work was supported by Research Institute of Petroleum Industry (RIPI).

Received : Oct. 3, 2011 ; Accepted : Dec. 2, 2013

### REFERENCES

- [1] Wu M.C., Corneille J.S., Estrada C.A, He J.W., Goodman D.W., Synthesis and Characterization of Ultra-Thin MgO Films on Mo (100), *Chem. Phys. Lett.*, **182**, p. 472 (1991).
- [2] Shukla S.K., Parashar G.K., Mishra A.P., Misra P., Yadav B.C., Shukla R.K., Bali L.M., Dubey G.C., Nano-Like Magnesium Oxide Films and Its Significance in Optical Fiber Humidity Sensor, *Sens. Actuators B*, **98**, p. 5 (2004).
- [3] Zhang L.D., Mo J.M., Nanometer Materials, *Science Press, Liaoning*, 303 (1994).
- [4] Sawai J., Kojima H., Igarashi H., Hashimoto A., Shoji S., Sawaki T., Hakoda A., Kawada E., Kokugan T., Shimizu M., Antibacterial Characteristics of Magnesium Oxide Powder, *World J. Microb. Biotechnol.*, **16**, p. 187 (2000).
- [5] Yamamoto O., Sawai J., Sasamoto T., Effect of Lattice Constant of Zinc Oxide on Antibacterial Characteristics, *Int. J. Inorg. Mater.* **2**, p. 451 (2000).
- [6] Koper O.B., Klabunde J.S., Marchin G.L., Klabunde K.J., Stoimenov P., Bohra L., Nanoscale Powders and Formulations with Biocidal Activity Toward Spores and Vegetative Cells of Bacillus Species, Viruses, and Toxins, *Curr. Microbiol.*, **44**, p. 49 (2002).
- [7] Stoimenov P.K., Klinger R.L., Marchin G.L., Klabunde K.J., Metal Oxide Nanoparticles as Bactericidal Agents, *Langmuir*, **18**, p. 6679 (2002).
- [8] Huang L., Li D., Lin Y., Wei M., Evans D.G., Duan X., Controllable Preparation of Nano-MgO and Investigation of Its Bactericidal Properties, *J. Inorg. Biochem.*, **99**, p. 986 (2005).
- [9] Han Y.J., Kim J., Stucky G.D., Preparation of Noble Metal Nanowires Using Hexagonal Mesoporous Silica SBA-15, *Chem. Mater.*, **12**, p. 2068 (2000).
- [10] Hu J., Odom T.W., Lieber C.M., Chemistry and Physics in One Dimension: Synthesis and Properties of Nanowires and Nanotubes, *Acc. Chem. Res.*, **32**, p. 435 (1999).
- [11] Chen C.C., Chao C.Y., Lang Z.H., Simple Solution-Phase Synthesis of Soluble CdS and CdSe Nanorods, *Chem. Mater.*, **12**, p. 1516 (2000).
- [12] Mohamed M.B., Ismail K.Z., Link S., El-Sayed M.A., Thermal Reshaping of Gold Nanorods in Micelles, *J. Phys. Chem.*, **102**, p. 9370 (1998).
- [13] Alavi M.A., Morsali A., Syntheses and Characterization of Mg(OH)<sub>2</sub> and MgO Nanostructures by Ultrasonic Method, *Ultrasonics Sonochemistry*, **17**, p. 441 (2010).
- [14] Takahashi N., Simple and Rapid Synthesis of MgO with Nano-Cube Shape by Means of a Domestic Microwave Oven, *Solid State Sci.*, **9**, p. 722 (2007).
- [15] Zhang H., Feng J., Wang J., Zhang M., Preparation of ZnO Nanorods Through Wet Chemical Method, *Mater. Lett.*, **61**, p. 5202 (2007).
- [16] Gericke M., Pinches A., Biological Synthesis of Metal Anoparticles, *Hydrometallurgy*, **83**, p. 132 (2006).

- [17] Esmaeili E., Khodadadi A., Mortazavi Y., Microwave- Induced Combustion Process Variables for MgO Nanoparticle Synthesis Using Polyethylene, *Journal of the European Ceramic Society*, **29**, p. 1061 (2009).
- [18] Kumari L., Vannoy C., Leblank R., Wang D.Z., Synthesis, Characterization and Optical Properties of Mg(OH)<sub>2</sub> Micro-/Nanostructure and Its Conversion to MgO, *Ceramics International*, **35**, p. 3355 (2009).